

DISTINCT TRANSVERSE EMITTANCE MEASUREMENTS OF THE PXIE LEBT*

R. D'Arcy[†], B. Hanna, L. Prost, V. Scarpine, A. Shemyakin, J. Steimel
Fermilab, Batavia, IL 60510, USA

Abstract

PXIE is the front-end test stand of the proposed PIP-II initiative i.e. the first step towards a CW-compatible, pulsed H- superconducting RF linac upgrade to Fermilab's injection complex. The test stand for this machine will be built step-wise; the Ion Source and Low-Energy Beam Transport (LEBT) are currently in place, with the RFQ and MEBT due for installation 2015.

The initial LEBT configuration under investigation in this paper is comprised of a D-Pace Filament-driven H- source and a single downstream solenoid, accompanied by a number of beam-diagnostic tools. The emittance studies expounded are performed via two methods: a position-angle phase-space sweep using an Allison-type emittance scanner; a solenoid corrector-induced transverse beam shift, impinging the bunch on an isolated, biased diaphragm. A detailed comparison of the two results is outlined.

INTRODUCTION

The proposed plan to upgrade Fermilab's injection complex consists of designing and building a CW SRF H- Linac. At its initial stage this is known as the Proton Improvement Plan II (PIP-II), to be used in pulsed mode. Front end components crucial for CW operation will be tested at an accelerator called, for historical reasons, PXIE [1], composed of a D-Pace [2] filament-driven H- ion source; a Low Energy Beam Transport (LEBT) section; a CW 2.1 MeV RFQ; a Medium Energy Beam Transport (MEBT) section; two SRF cryomodules (HWR and a SSR1); a High Energy Beam Transport (HEBT); and a beam dump. Figure 1 shows a schematic of the proposed beamline. The content of this paper will concern itself with the initial beam diagnostic results of the LEBT, namely the emittance measurements with two methods: Allison scanner and solenoid scans at the same beam conditions of, in part, a current of 2 mA. For a more detailed outline of the experiment, and its current status, please refer to [3].

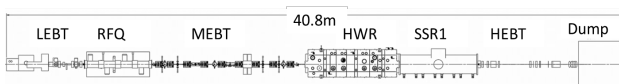


Figure 1: The proposed PXIE beamline.

* Operated by Fermi Research Alliance, LLC, under Contract DE-AC02-07CH11359 with the U.S. DOE.

[†] rtpdarcy@fnal.gov

LOW ENERGY BEAM TRANSPORT

The LEBT section of PXIE began with installation of the 30 keV H- ion source, producing beam in either pulsed (0.001 – 16 ms at 10 Hz) or CW mode with a beam current of 0.1 – 10 mA. Since then the beamline has been installed incrementally with the addition of a first solenoid, along with beam diagnostic tools, at the start of 2014. Once this initial layout was commissioned, the addition of two further downstream solenoids was completed in mid-2014. The data taking and results included in this paper are for the initial one-solenoid layout previously described, displayed in more detail in Fig. 2.

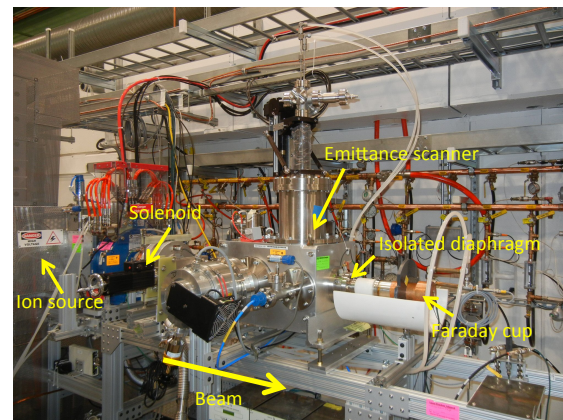
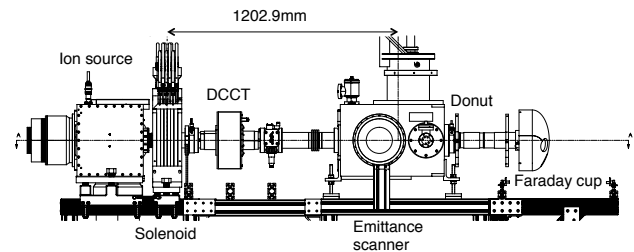


Figure 2: A schematic and photograph of the LEBT section constructed at the time of data taking for this paper.

ALLISON EMITTANCE SCANNER

The main tool to measure the beam emittance in the layout shown in Fig. 2 is the Allison Emittance Scanner. The Allison scanner was designed and built in collaboration with SNS and is based upon the original proposal in 1983 by P. Allison et al. [4]. The pictorial representation of the scanner, copied from [5], is shown in Fig. 3. The scanner measures the phase portrait of the beam in one dimension (vertical in the reported case). The scanner assembly consists of two slits, a Faraday cup with a suppressor electrode, and two de-

flexion plates placed symmetrically with respect to the slits. The spatial coordinate of a phase slice is determined by the position of the entrance slit and is adjusted by a step motor moving the entire assembly. The slice angle is determined by the voltage V applied between plates. In approximation of a negligible slit size, particles can pass through both slits only when their initial angle x' with respect to the scanner axis is

$$x' = \frac{VL}{4g_e U}, \quad (1)$$

where L is the effective length of the plates, g_e is the effective gap between the plates, and qU the energy of the ion. For the PXIE LEBT Emittance Scanner (with voltage applied symmetrically to each plate $V/2 = 1000$ V, $L = 96$ mm, $g_e = 8.9$ mm, and $U = 30$ kV) the scanner can operate over an angular range of ± 180 mrad and a spatial range of ± 30 mm.

The scanner's Faraday cup signal goes to a 16-bit, ± 10 V ADC, which for the primarily unipolar signal has a dynamic range of 3×10^4 . The secondary electrons from the Faraday cup are suppressed by the field of the suppressor electrode, typically biased at -100 V. The voltage of the deflecting plates is swiped at 10 Hz.

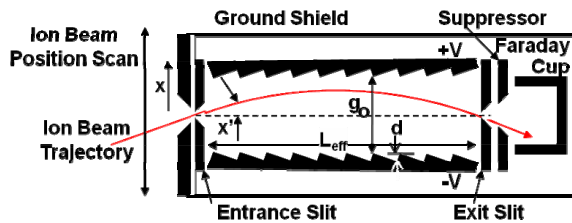


Figure 3: Pictorial representation of the Allison scanner, with a demonstration of the bending properties of the electric plates [5]. The deflecting plates are stair-cased with a depth d to prevent impacting particles from being scattered into the back slit.

Ultimate spatial resolution can be determined by the step size of the motor drive (0.01 mm) or by the entrance slit size (0.2 mm). The angular resolution is dictated by the slit size. As a measure of the angular resolution one can consider the RMS size of a distribution that would be measured with these slits for a beam slice with zero angular scatter. For the size of the second slit of 0.5 mm, such estimation gives 1.5 mrad. In practice, however, the granularity of the measured phase portraits was determined by the need for a reasonably low measuring time (approx. 3 mins) for a typical scan with 31 points over a 30 mm shift by 61 points over a 60 mrad angle sweep.

Note that the main modification of the PXIE emittance scanner with the previous SNS design [5] is an added capability of operating in DC mode. For that, the entrance slits are made of the Molybdenum alloy TZM and bolted to the water-cooled stainless steel body with a Carbon foil in

between. Simulations¹ predict a safe operation with a DC 10 mA (300 W) beam focused to a spot with RMS size as low as 3 mm. So far, the minimum size in measurements of 10 mA beam was 3 mm RMS without any indications of performance deterioration.

Calibration

The spatial calibration for the emittance scanner was performed using a spring gauge, with a resolution of $10 \mu\text{m}$, placed at the top of the shaft. This measured the movement of the scanner box as related to the number of steps made by the motor. The conversion of motor steps to distance travelled was found to be accurate and reproducible to less than a percent.

Uncertainty in the angular calibration is related to the values in Eq. 1. This model includes the calibration of the plate voltage and ion energy as well as the relationship between the voltage and the electric field integral along the ion trajectory (the ratio of L/g_e). However, we found a way of a direct calibration, which uses the dipole correctors built into each solenoid for shifting the beam in two orthogonal directions. The fields of the correctors have been measured, and their deflecting properties were independently verified using beam shifting with respect to the donut (see the next section) and using the bottom part of the emittance scanner as a scraper. It allowed finding combinations of the currents in two correctors (at a given solenoid current) that would kick the beam either horizontally or vertically by a known amount (within 1%). A vertical kick results in both a shift Δx of the beam centroid at the location of the emittance scanner slit and a change of the angle centroid by

$$\Delta x' = \frac{\Delta x}{L_{\text{sol} \rightarrow \text{es}}}, \quad (2)$$

where $L_{\text{sol} \rightarrow \text{es}}$ is the distance between the centre of the correctors and the entrance slit.

Substituting initially the effective values of the gap and length in Eq. 1 by their geometrical values, and assuming that the ion energy and the plate voltage follow exactly to settings, one can record the spatial and angular positions of the beam centroid as measured by the emittance scanner at various vertical kicks. Comparing the slope of the measured line $\Delta x' = f(\Delta x)$ with the known value of $L_{\text{sol} \rightarrow \text{es}} = 1.203$ m, one can correct the coefficient used by the program to make them agree (Fig. 4). The uncertainty of angle calibration with this procedure is determined primarily by the scatter of data in Fig. 4 and is approx. 2%.

Pulse Analysis

The PXIE Ion Source is CW but, due to the introduction of a modulator at the extraction electrode, the beam may be pulsed with duration of 0.001-16 ms and frequency up to 60 Hz. The pulse mode is preferable at the commissioning stage to decrease the chances of damage to the machine.

¹ The scanner design and simulations were made by M. Alvarez and J. Gaynier.

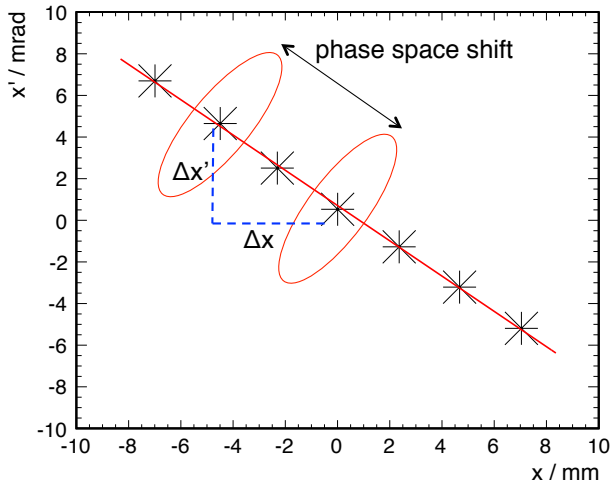


Figure 4: Phase space shifts of the centroids caused by the vertical kicks by the solenoid dipole correctors.

The emittance scanner analysis package can analyse both DC and pulsed beams, breaking down the structure of each timing window into individual time slices. Each pulse is sampled at a rate of 1 MHz so, for example, a slice size of 10 μs would produce an array of data averaged across 10 measurements, thus reducing the statistical noise between pulses. The plot in Fig. 5 demonstrates the evolution of both the RMS beam size and normalised emittance across a 400 μs pulse with 25 μs slices. In this figure both parameters plateau at approximately 300 μs suggesting a neutralisation time slightly shorter than this. All data reported further were taken at the back end of the 400 μs pulse.

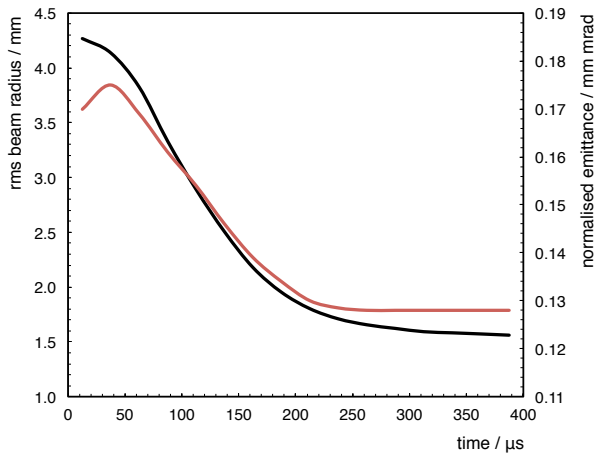


Figure 5: A graphical representation of the evolution of the RMS beam size (black) and normalised emittance (red) along a 400 μs, 5 mA H- pulse.

Initial Results

The emittance scanner is controlled by a Labview [6] package which operates the HV supplies and stepper driver and reads the thermocouples, Faraday cup, etc. After calibra-

tion of the emittance scanner, data were parsed into bespoke analysis software. In the pulsed mode, the instrumental background is subtracted using the data recorded before the pulse triggers - the default time window being 100 μs. In addition, a user-specified cut (in percents of the maximum signal) is applied to remove from the signal a beam-related background that might not come directly from the primary ions. After this threshold cut a centering routine was utilised. Figure 6 gives an example of a 2 mA beam phase portrait after applying such a procedure, as well as the collapsed profile plots for both the spatial and angular axes. The normalised RMS emittance value (with a 1% threshold cut) for this distribution is $\epsilon_{RMS} = 0.074 \pm 0.002$ mm.mrad. For a perfectly double-Gaussian beam the RMS and the 39% emittance are equal. The 39% emittance for this distribution is $\epsilon_{39\%} = 0.053 \pm 0.002$ mm.mrad. The enlarged RMS emittance is due to the S-shaped phase space structure, with tails pulled off from the core. Such S-shaped emittances are normal for low-energy ion beams, where aberrations in the extraction system and lenses cause the outer part of the beam to over focus [7].

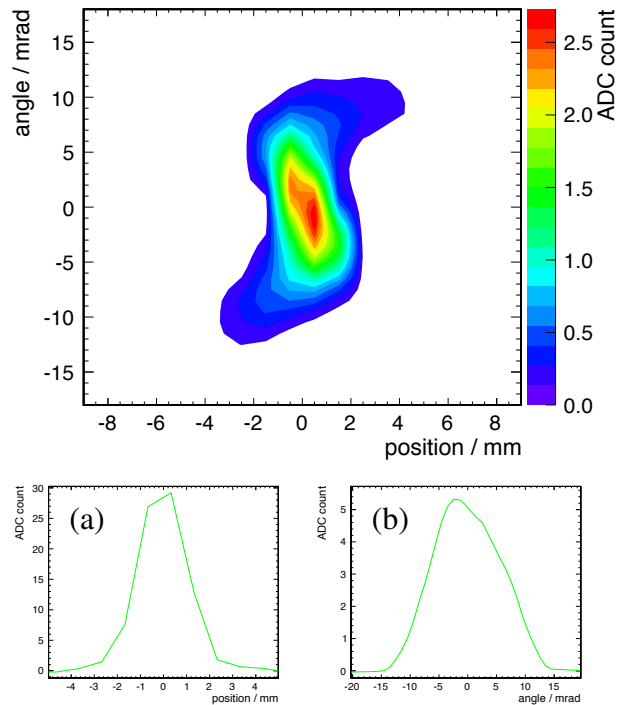


Figure 6: The phase space, as recorded by the Allison scanner, for a 2mA H- beam. Also shown are the collapsed profiles of the a) x-, and b) x'-axes. The background cut is 1%.

Core Emittance Calculation

A widely used procedure to characterise the beam core e.g. in 1D spatial distribution, is to fit its central part to a Gaussian curve. The analog of such procedure for a phase portrait is to fit its central area with a function that is Gaus-

sian in both angular and spatial dimensions. The procedure was implemented as follows:

- Twiss parameters α , β , and γ are calculated from the recorded phase space data using 0% cut,
- Action [8] is calculated for each (x, x') data point as

$$J = \frac{1}{2} (\gamma x^2 + \alpha x x' + \beta x'^2) \quad , \quad (3)$$

- The data points are ordered according to their action. The percentage of beam outside of a given action is calculated as a function of action,
- The portion of the function corresponding to low action is fitted to

$$N(J) = e^{-\frac{J}{\epsilon_{\text{core}}}} \quad , \quad (4)$$

with ϵ_{core} as the only free parameter, which we will refer to as the core emittance.

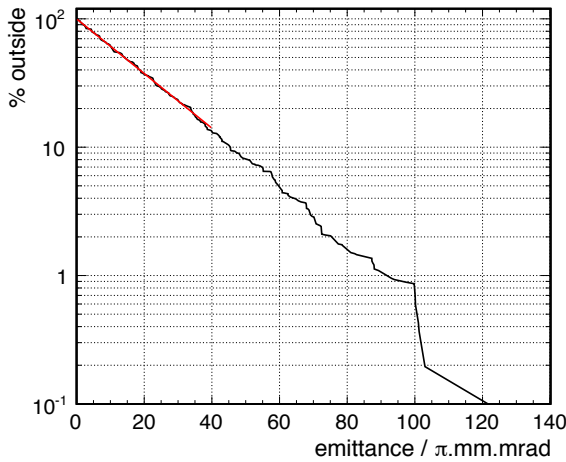


Figure 7: The percentage of beam outside a given emittance value for the phase space distribution of Fig. 6. An exponential fit to the initial straight section yields a value for the core emittance.

An example of such a plot and fit can be seen in Fig. 7. The value of the fitted core emittance $\epsilon_{\text{core}} = 0.082 \pm 0.003$ mm.mrad is 10% larger than the RMS emittance calculated in the previous section. This is due to the beam phase tails falling faster than assumed by the double-Gaussian distribution and is related to a non-Gaussian spatial profile at the ion source. We find the notion of a core emittance useful to describe the brightness of the beam core because it is significantly more rigorously defined and depends less on the choice of the threshold cut than the RMS emittance, as illustrated by Fig. 8.

SOLENOID SCAN METHOD

An alternative way to measure the beam emittance is to measure the beam size at various solenoid currents and compare these data with a propagation model. In the setup of Fig. 2, the beam size measurement can be performed

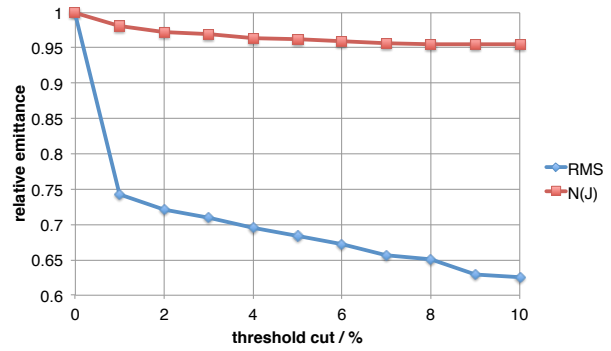


Figure 8: A graphical comparison of the evolution of both the RMS and core emittance across a range of threshold cuts, each normalised by their respective maximum value.

using the dipole correctors incorporated into the solenoid design and an electrically isolated, 18 mm ID diaphragm (also known as the ‘donut’) in front of a Faraday cup. When the beam is moved by the dipole correctors across the donut, it successively impinges one side of the donut, passes into the Faraday cup, and comes to the opposite side of the donut (Fig. 9). If the scan trajectory passes the donut centre, fitting of it simultaneously gives the information about calibration of the corrector strength (shift per Ampere), position of the centre in the direction of the scan, and the beam size. Strictly speaking, fitting requires solving an integral equation to reconstruct the beam density distribution. To simplify the procedure, fitting was done assuming either constant density or Gaussian distribution. The difference in the RMS beam size reconstructed with these two fits did not exceed 20%. For the Gaussian case, the portion of the beam current that passes to the Faraday cup $I(x, R, \sigma)$ is fitted as follows:

$$I(x, R, \sigma) = \frac{1}{\pi} \int_{\frac{-R-x}{\sqrt{2}\sigma}}^{\frac{R-x}{\sqrt{2}\sigma}} e^{-u^2} \left[\sqrt{\frac{R^2}{2\sigma^2} - \left(u + \frac{x}{\sqrt{2}\sigma}\right)} \right] du \quad , \quad (5)$$

where R is the donut radius, x the centre position of the beam relative to the centre of the donut, and σ the RMS beam size. By centering the beam by hand before making a corrector scan the only free parameter from the fit is the RMS beam size.

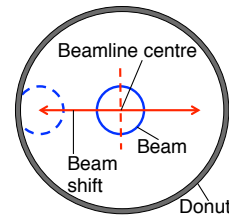


Figure 9: Illustration of the beam motion across the donut.

An example of a corrector scan can be seen in Fig. 10, with the fit denoted by the red curve. The beam size resulting from the fit is $\sigma = 1.35$ mm. This process may then be repeated for a series of solenoid currents creating a relation

between the solenoid current and the RMS beam size. An example of this relation can be seen in Fig. 11.

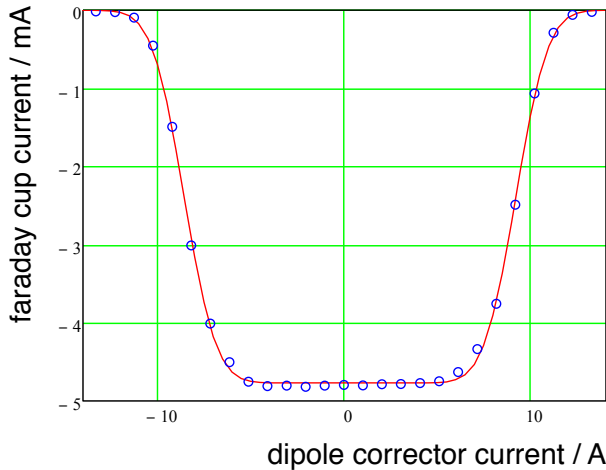


Figure 10: Beam current reaching the Faraday cup versus the dipole corrector current. Blue circles are measurements, and the solid red curve is the fit. Beam current is 2 mA. The beam is preliminarily centered in the opposite direction. The data were recorded at the end of 0.4 ms pulse.

For extracting the emittance we used the simplest propagation model that includes only a solenoid, approximated by a thin lens with the equivalent dependence of the focusing strength on the solenoid current $f(I_{sol}) = \frac{k}{I_{sol}^2}$, and a drift space with no space charge

$$\sigma^2 = \sigma_0^2 + 2\sigma_0\sigma'_0L + \left(\frac{\epsilon^2}{\sigma_0^2} + \sigma_0'^2\right)L^2 \quad (6)$$

where L is the distance between the lens and the centre of the donut, and $\sigma'_0 = \frac{\sigma_0}{f(I)} - \sigma'$. The free parameters of this fit are therefore σ_0 , σ'_0 , and ϵ . The emittance obtained from such a fit to data in Fig 11 is $\epsilon = 0.084$ mm.mrad. The propagated statistical error is several percent, but the uncertainty related to the model itself is significantly larger, probably $\sim 10\%$. The emittance value agrees with that derived for a 2 mA beam using the emittance scanner.

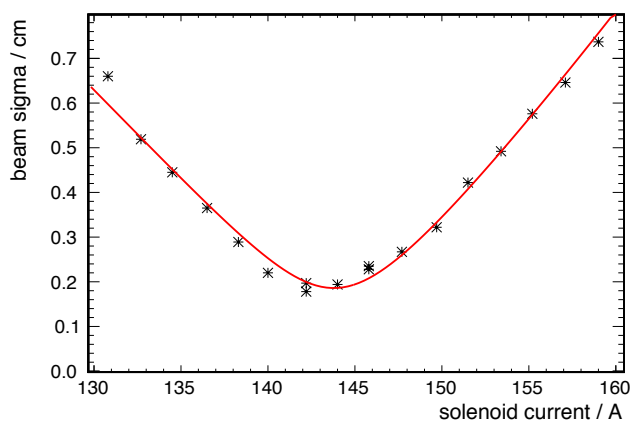


Figure 11: Beam size as a function of solenoid current with a fit used to derive the emittance of the beam.

CONCLUSIONS AND PLANS

1. Two methods of measuring the beam emittance have been successfully commissioned and used at the PXIE LEBT one-solenoid assembly in a long-pulse mode, with an Allison-type emittance scanner and the solenoid scan, which we consider being complimentary. The solenoid scan method doesn't require sophisticated equipment and the emittance value can be measured for any direction. On the other hand, the emittance scanner provides a detailed phase portrait, and its emittance figure doesn't depend on the pre-chosen distribution model. The results obtained with these two methods agree within the error margin.

2. The angle measurement of the emittance scanner was calibrated to 2% accuracy.

3. The introduced notion of the core emittance allows estimating the brightness of the beam core in a manner weakly affected by the choice of the threshold cut.

The commissioned diagnostic tools are now used in the three-solenoid beamline both in pulse- and DC-modes to optimise the beam for future injection into the RFQ in 2015.

ACKNOWLEDGEMENTS

Thanks go to Martin Stockli, Willem Blokland, et al. from SNS at ORNL who designed the original Allison scanner, wrote the Labview code to operate the machine, and provided technical knowledge during all phases of commissioning. Thanks also go to Matt Alvarez, Sali Sylejmani, and Jared Gaynier for building and installing the machine, simulating beam-induced thermal effects, and constantly providing expert mechanical support. Finally the authors of the paper would like to thank Dave Slimmer for his work with updating the Labview code.

REFERENCES

- [1] V. Lebedev *et al.*, *An 800 MeV Superconducting Linac to Support Megawatt Proton Operations at Fermilab*, Proc. of LINAC14, Geneva, Switzerland (2014), THIOA05.
- [2] D-Pace, Inc. <http://www.d-pace.com>.
- [3] A. Shemyakin *et al.*, *Status of the Warm Front End of PXIE*, Proc. of LINAC14, Geneva, Switzerland (2014), THPP056.
- [4] P. Allison, J. Sherman, D. Holtkamp, *An emittance scanner for intense low-energy ion beams*, IEEE Trans. Nucl. Sci. NS-30 (1983).
- [5] M. Stockli *et al.*, *Low Energy Emittance Studies with the new Allison Emittance Scanner*, Proc. of PAC09, Vancouver, Canada (2009), TH6REP012.
- [6] National Instruments, Inc. <http://www.ni.com/labview/>
- [7] M. Stockli, *Measuring and Analyzing the Transverse Emittance of Charged Particle Beams*, Proc. of BIW06, Fermilab, Batavia, USA (2006), CP868.
- [8] S.Y. Lee, *Accelerator Physics*, World Scientific, Singapore (1999), p.51.